Applied Mathematics and Computation 382 (2020) 125325

Contents lists available at ScienceDirect

Applied Mathematics and Computation

journal homepage: www.elsevier.com/locate/amc

Green's function and surface waves in a viscoelastic orthotropic FGM enforced by an impulsive point source

Raju Kumhar[a,*], Santimoy Kundu[a], Deepak Kr. Pandit[a], Shishir Gupta[a]

Department of Mathematics and Computing, Indian Institute of Technology (Indian School of Mines), Dhanbad Jharkhand 826004, India

ARTICLE INFO

Article history:
Received 5 June 2019
Revised 4 September 2019
Accepted 19 April 2020

Keywords:
Shear wave (SH-wave)
Heterogeneity
Voigt-type viscoelastic
Functionally graded material
Dispersion equation
Attenuation coefficient

ABSTRACT

Analytical and numerical approach are taken into consideration to analyze the propagation behavior of horizontally polarized shear surface waves (SH-wave) influenced by an impulsive point source in pre-stressed heterogeneous Voigt-type viscoelastic orthotropic functionally graded (FGM) layered structure. The mechanical properties of the material of viscoelastic functionally graded layer vary with respect to a certain depth as a hyperbolic function, while it varies as a quadratic function for the viscoelastic functionally graded half-space. The complex wave velocity of SH-wave has been achieved by the method of Green's function and Fourier transformation under the appropriate boundary conditions of the adopted model. The derived wave velocity of SH-waves has been reduced to the classical equation of Love wave when both the viscoelastic orthotropic FGM layer and half-space are considered to be homogeneous isotropic elastic, as depicted in the section of particular cases and validation. Moreover, numerical computation of the obtained velocity equation has been performed and the substantial effects of viscoelasticity and heterogeneity on phase velocity as well as attenuation coefficient for both the cases of absence and presence of initial stress in the media have been perceived by the means of graphs. The final results of this work may be relevant to understand the useful information of SH-wave propagation in the considered layered structure.

1. Introduction

The study of seismic waves is one of the most important phenomena for understanding the surface and internal structure of the Earth. Geophysicists and seismologists analyses the traversal behavior of seismic waves such as Rayleigh wave, SH-wave, torsional wave, P-wave, and S-wave, etc. in order to model Earth's interior and also to investigate the nature of earthquake sources with the ultimate goal of mitigation and eventually controlling the phenomena. These seismic waves behave differently when they pass through different types of material with different physical states (for example, solid, molten, semi-molten). The behaviour of these seismic waves such as their strength, and the direction form where they are originated are recorded at the seismic stations and utilised by geologists for better understanding of the Earthquake as well as Earth's crust. A detailed theoretical information as well as applications regarding the analysis of seismic waves in layered media are provided in well established literatures (Ewing et al.[1], Love [2], Gubbins [3] and Pujol [4])

Many researchers in the existing literatures (Vinh et al. [5], Gourgiotis and Georgiadis [6], Dutta [7], Singh [8], Zhu et al. [9] and Pang et al. [10]) have considered the seismic wave propagation in a model constituted of isotropic elastic and ho-

* Corresponding author.
E-mail address: rajukumhar.2016dr0006@am.ism.ac.in (R. Kumhar).

https://doi.org/10.1016/j.amc.2020.125325
0096-3003/

mogeneous material. Although, isotropic material is the basics constituent for anisotropic and smart material, it is regarded as ideal case. Furthermore, it is to be noted that the Earth is composed of different layers with different material and geological characteristics that is highly responsible for large alteration and acute changes in their material properties. These variations in elastic bodies contribute to the heterogeneity of the medium and have prominent influence on the behaviour of seismic waves. The mechanical behaviour of natural geomaterials, such as natural clay deposits built up by sedimentation and subsequent consolidation, or rock masses cut by discontinuities, etc., may display both heterogeneity and anisotropic. Orthotropic materials is the subset of anisotropic material which has different material properties along three mutually orthogonal directions. Wood, composites, many crystals, and rolled metals fall under the categories of orthotropic material. Destrade [11] derived the existence of surface waves in orthotropic incompressible materials. Abd-Alla and Ahmed [12] studied the Love wave passes through the orthotropic elastic medium under initial stress. Many seismologists and researchers mostly prefer the anisotropic and heterogeneous coupled structure to analyze the influence of heterogeneity on surface wave propagation and in order to gain deep insight about the Earth's internal structure. Wilson [13] was the first to describe the traversal characteristics of surface waves through heterogeneous layered structure. Dey et al. [14] delineated the traversal of torsional surface wave in quadratic and exponential functioned heterogeneous layer. In addition to heterogeneity and anisotropy, the initial stress is another trivial property of an elastic body. Various factors like overburdening of layers, gravitational field, atmospheric pressure, and slow process of creep etc. are responsible for the generation of initial stress. These stresses are highly responsible for the instability arising in ground which leads to generation of earthquakes. Therefore, it is obligatory to discuss the traversal characteristics of elastic surface waves in an initially stressed layered structures. Biot [15] described the impact of initial stress and gravitational field on elastic body in detail. Saha et al. [16] examined the effect of compressive and tensile stresses on the propagation of torsion surface waves. They noted that the initial stresses (compressive or tensile) have a significant impact on the speed of surface waves. Since the earth has an initially stressed elastic body, it is more realistic to consider the initial stress effect. Many authors such as Kundu et al. [17], Ke et al. ([18], [19]), Wang et al. [20] and Abd-Alla et al. [21] have produced their valuable view on the influence of heterogeneity and initial stress on the traversal of seismic surface waves.

Viscoelasticity play a major role in the motion and behaviour of the tectonic plates, the plates floating on the Earth's mantle and moving independently are responsible for vibration, volcanoes and earthquakes, etc. Mechanical materials such as sediments, salt and coal tar which are buried under the Earth's surface can be modelled as viscoelastic material. High internal damping is unique characteristics of the viscoelastic materials leading to the damping of waves and vibrations created during an artificial exploration and earthquake. Consequently, these viscoelastic materials are proficiently utilized in vibration and noise control, position and shape control, non-destructive evaluation and health monitoring systems, and in many branches of engineering. Carcione [22] was the first to investigate the propagation of seismic waves not only by anisotropy but also by the intrinsic viscosity of the media. In addition, Borcherdt [23] and Carcione [24] discussed the traversal of Rayleigh-type waves in a viscoelastic medium. Presently, Maity et al. [25] have published a paper on torsional wave vibrations through viscoelastic fiber-reinforced medium. They have studied the internal friction (viscoelasticity) has pronounced impact on the dispersion and attenuation (arises due to a complex wave number) of torsional waves.

Due to the gradual change in material properties, the functionally graded materials have attracted much more attention in recent years with their increasing use in various applications. The current areas of applications include aerospace, automobile, electrical/electronic, energy and marine etc. Similarly, these are currently used in many industries and will also be used in many applications in the future. Therefore, it's a vital part to study the traversal of seismic wave problems in such type of materials. Hence, we have considered here the FGM composed of orthotropic material with Voigt-type viscoelastic under initial stress. The study of seismic wave problems through the FGM plates and FGPM plates has been discussed by many researchers, some of whom are Kong et al. [26], Paulino and Jin [27], Yu and Zhang [28], Qian et al. [29] and Yu et al. [30]. In addition to that, Ren et al. [31], Li et al. [32], Qian et al. [33] and Liu and Wang [34] also studied the traversal of Love wave in FGM structure. They examined in detail the effects of proposed parameters on the dispersion curves such as gradient coefficients, piezoelectric and dielectric constants. Keeping these facts in mind, authors have made an effort to undertake the present study of the shear wave propagation due to impulsive point source in pre-stressed heterogeneous viscoelastic orthotropic FGM layer and half-space, which has not been attempted by any authors till date.

Almost all authors have applied the conventionally developed methods such as separation of variables, variational method, integral transformation, etc., in order to solve the equations of motion for any material medium of the Earth's crust. But in this problem, the technique of Green's function and Fourier transformation have been applied to solve the governing equations associated with the concerned medium. The main reason behind applying this method is that the Green's function imparts a phenomenal elucidation of behavior related to forces focused on a point which works as a disturbance source. These forces are formed by a unit impulsive force in time and space, which can be mathematically expressed with the help of Dirac delta function. Green's function exhibits a crucial role for solving the elastodynamic problems related to the point source or an impulse force responsible for wave movements in material medium. In the field of science and technology, the applications of Green's function are related with the Initial and Boundary Value Problems, Kirchhoff's Diffusion Equation, Wave Equation, Helmholtz's Equation and Diffraction Theory etc. So far, only a few research work based on the technique of such functions has been carried out, which is attracting the attention of researchers and practitioners in the area of mechanics of solids, applied mathematics, applied physics, material science and mechanical engineering. The authors Assari and Dehghan ([35], [36], [37]) have solved two dimensional Laplace's equation with the aid of Robin boundary conditions based on the boundary integral equations using Green's function technique.

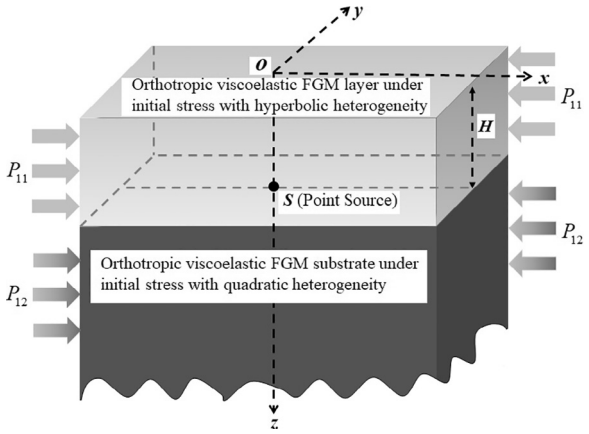

Fig. 1. Structure of viscoelastic orthotropic FGM layered Earth model.

The main concern of the present work is to analyze the propagation characteristics of the SH-wave influenced by an impulsive point source in an orthotropic viscoelastic FGM finite layer overlying orthotropic viscoelastic FGM semi-infinite medium under the effect of initial stresses. Closed form of complex wave velocity equation of shear surface wave has been obtained with the help of Fourier transform and Green's function technique. The phase velocity and attenuation curves against wave number is plotted from real and imaginary terms of the obtained wave velocity equation. In the numerical section, the crucial observations and impact on phase velocity and attenuation coefficient against wave number have been discussed by varying values of the proposed parameters such as heterogeneities and viscoelasticity factors. In addition to that, a comparative study is point out to examine the effect of influencing parameters for both the cases of presence and absence of initial stress on the traversal of SH-waves in considered model.

2. Formulation of physical model and its solution

In the context, consider a semi-infinite pre-stressed viscoelastic orthotropic functionally graded material covered with pre-stressed viscoelastic orthotropic FGM layer of finite width H under the different kind of heterogeneities. A rectangular Cartesian frame $Oxyz$ is chosen in order to represent our model where the origin O is taken at the upper surface. Propagation of surface shear wave (SH-wave) is taken along x-axis i.e. the horizontal direction whereas the alignment of z-axis is in vertically downward direction, as depicted in Fig. 1. The source of disturbance S is considered at a common interface of the adopted model. The orthotropic viscoelastic layer and semi-infinite medium are defined as the region $0 \le z \le H$ and $H \le z < \infty$, respectively.

The orthotropic viscoelastic constitutive equation can be written in the following form (Yu et al. [30])

$$\left.\begin{aligned}
\tau_{11}^{l} &= \mu_{11}^{l} e_{11} + \mu_{12}^{l} e_{22} + \mu_{13}^{l} e_{33},\\
\tau_{22}^{l} &= \mu_{21}^{l} e_{11} + \mu_{22}^{l} e_{22} + \mu_{23}^{l} e_{33},\\
\tau_{33}^{l} &= \mu_{31}^{l} e_{11} + \mu_{32}^{l} e_{22} + \mu_{33}^{l} e_{33},\\
\tau_{12}^{l} &= 2\mu_{66}^{l} e_{12},\\
\tau_{23}^{l} &= 2\mu_{44}^{l} e_{23},\\
\tau_{31}^{l} &= 2\mu_{55}^{l} e_{31},
\end{aligned}\right\} \quad l = 1, 2 \tag{1}$$

where $e_{ij} = \frac{1}{2}\left(u_{i,j} + u_{j,i}\right)$ and τ_{ij}^{l} are the components infinitesimal strain and incremental stress, respectively. and

$$\mu_{ij}^{l} = \widehat{\mu}_{ij}^{l} + \widehat{\eta}_{ij}^{l} \frac{\partial}{\partial t} \tag{2}$$

In the considered layered Earth model, the variation of mechanical properties such as elastic parameter, viscoelastic coefficient, initial stress and density for orthotropic viscoelastic FGM layer and half-space have been adopted as follows:

$$\widehat{\mu}_{ij}^{1} = \mu_{ij}^{11}\cosh^2(\gamma z), \quad \widehat{\eta}_{ij}^{1} = \eta_{ij}^{11}\cosh^2(\gamma z), \quad P_1 = P_{11}\cosh^2(\gamma z), \quad \rho_1 = \rho_{11}\cosh^2(\gamma z) \tag{3}$$

and

$$\widehat{\mu}_{ij}^{2} = \mu_{ij}^{12} + \varepsilon(z-H)^2, \quad \widehat{\eta}_{ij}^{2} = \eta_{ij}^{12} + \varepsilon(z-H)^2, \quad P_2 = P_{12} + \varepsilon(z-H)^2, \quad \rho_2 = \rho_{12} + \varepsilon(z-H)^2 \tag{4}$$

Using the Eqs. (3) and (4) in Eq. (2), we have

$$\left.\begin{aligned}\mu_{ij}^{1} &= \left(\mu_{ij}^{11} + \eta_{ij}^{11}\frac{\partial}{\partial t}\right)\cosh^2(\gamma z)\\ \rho_1 &= \rho_{11}\cosh^2(\gamma z)\\ P_1 &= P_{11}\cosh^2(\gamma z)\end{aligned}\right\} \tag{5}$$

and

$$\left.\begin{aligned}\mu_{ij}^{2} &= \left(\mu_{ij}^{12} + \eta_{ij}^{12}\frac{\partial}{\partial t}\right) + \left(1 + \frac{\partial}{\partial t}\right)\varepsilon(z-H)^2\\ \rho_2 &= \rho_{12} + \varepsilon(z-H)^2\\ P_2 &= P_{12} + \varepsilon(z-H)^2\end{aligned}\right\} \tag{6}$$

where, μ_{ij}^{11}, η_{ij}^{11}, ρ_{11}, P_{11} and γ are elastic constant, viscoelastic coefficient, density, initial stress and heterogeneity parameter for viscoelastic layer. Similarly, μ_{ij}^{12}, η_{ij}^{12}, ρ_{12}, P_{12} and ε are elastic constant, viscoelastic coefficient, density, initial stress and heterogeneity parameter for viscoelastic half-space.

Horizontal polarized shear surface waves (SH-wave) conditions : Let the displacement components for the Voigt-type viscoelastic orthotropic FGM upper layer and lower semi-infinite medium be (u_1, v_1, w_1) and (u_2, v_2, w_2), respectively. Hence the characteristics of shear wave propagation are given by

$$u_i = w_i = 0, \quad \frac{\partial}{\partial y} = 0 \quad \text{and} \quad v_i = v_i(x, z, t), \quad i = 1, 2 \tag{7}$$

2.1. Solution for the bounded medium

If the medium is affected by a point source, the governing equations are

$$\tau_{ij,j}^{1} + F_i' = \rho_1 \ddot{u}_i, \tag{8}$$

where ρ_1 and τ_{ij}^{1} are the density and components of stress, respectively; F_i' are the forces at a point of the upper layer where the elastic displacements are evaluated.

The dynamic equation of SH-wave in Voigt-type viacoelastic orthotropic functionally graded layer under the initial stress is

$$\frac{\partial \tau_{12}^{1}}{\partial x} + \frac{\partial \tau_{23}^{1}}{\partial x} - P_1\frac{\partial w_z}{\partial x} - \rho_1\frac{\partial^2 v_1}{\partial t^2} = 4\pi\sigma_1(r, t) \tag{9}$$

where P_1, w_z and $\sigma_1(r, t)$ are initial stress, rotational component and force density of the medium, respectively.

Using Eqs. (1) and (5) in Eq. (9), we get

$$\frac{\partial}{\partial x}\left[\left(\mu_{66}^{11} + \eta_{66}^{11}\frac{\partial}{\partial t}\right)\cosh^2(\gamma z)\frac{\partial v_1}{\partial x}\right] + \frac{\partial}{\partial z}\left[\left(\mu_{44}^{11} + \eta_{44}^{11}\frac{\partial}{\partial t}\right)\cosh^2(\gamma z)\frac{\partial v_1}{\partial z}\right] - \frac{P_{11}}{2}\cosh^2(\gamma z)\frac{\partial^2 v_1}{\partial x^2} - \rho_{11}\cosh^2(\gamma z)\frac{\partial^2 v_1}{\partial t^2} = 4\pi\sigma_1(r, t) \tag{10}$$

The force density $\sigma_1(r, t)$ are formed by a unit impulsive force in time and space which can be mathematically expressed with the help of Dirac delta function at the point source as

$$\sigma_1(r, t) = \delta(x)\delta(z - H)e^{i\omega t} \tag{11}$$

where ω is an angular frequency.

For a shear wave travelling in the positive direction of x-axis, we may assume

$$v_1(x, z, t) = e^{i\omega t}v_1(x, z) \tag{12}$$

Substituting the Eqs. (11) and (12) in Eq. (10), we have

$$\left(\frac{\bar{\mu}_{61}}{\bar{\mu}_{41}} - \frac{P_{11}}{2\bar{\mu}_{41}}\right)\frac{\partial^2 v_1}{\partial x^2} + \frac{\partial^2 v_1}{\partial z^2} + \frac{2\gamma\sinh(\gamma z)}{\cosh(\gamma z)}\frac{\partial v_1}{\partial z} + \frac{\rho_{11}}{\bar{\mu}_{41}}\omega^2 v_1 = \frac{4\pi\delta(x)\delta(z - H)}{\bar{\mu}_{41}\cosh^2(\gamma z)} \tag{13}$$

where

$$\bar{\mu}_{61} = \mu_{66}^{11} + i\omega\eta_{66}^{11} \quad \text{and} \quad \bar{\mu}_{41} = \mu_{44}^{11} + i\omega\eta_{44}^{11}$$

We use the following transformation to eliminate the term $\frac{\partial v_1}{\partial z}$ in Eq. (13)

$$v_1(x, z) = V_1(x, z)/\cosh(\gamma z) \tag{14}$$

Using the Eq. (14) in Eq. (13), we have

$$\left(\frac{\bar{\mu}_{61}}{\bar{\mu}_{41}}-\frac{P_{11}}{2\bar{\mu}_{41}}\right)\frac{\partial^2 V_1}{\partial x^2}+\frac{\partial^2 V_1}{\partial z^2}+\left(\frac{\rho_{11}}{\bar{\mu}_{41}}\omega^2-\gamma^2\right)V_1=\frac{4\pi\delta(x)\delta(z-H)}{\bar{\mu}_{41}\cosh(\gamma z)} \tag{15}$$

Introduce the Fourier transform $\bar{V}_1(\xi,z)$ of $V_1(x,z)$ as

$$\bar{V}_1(\xi,z)=\frac{1}{2\pi}\int_{-\infty}^{\infty}e^{i\xi x}\,V_1(x,z)dx$$

and the inverse Fourier transform is

$$V_1(x,z)=\int_{-\infty}^{\infty}e^{-i\xi x}\,\bar{V}_1(\xi,z)d\xi$$

Applying the Fourier transformation in Eq (15), we have

$$\frac{d^2\bar{V}_1}{dz^2}-\kappa_1^2\bar{V}_1=4\pi\sigma_1(z) \tag{16}$$

where

$$\kappa_1^2=\left(\frac{\bar{\mu}_{61}}{\bar{\mu}_{41}}-\frac{P_{11}}{2\bar{\mu}_{41}}\right)\xi^2-\lambda_1^2,\qquad \lambda_1^2=\left(\frac{\rho_{11}}{\bar{\mu}_{41}}\omega^2-\gamma^2\right) \tag{17}$$

and

$$4\pi\sigma_1(z)=\frac{2\delta(z-H)}{\bar{\mu}_{41}\cosh(\gamma z)} \tag{18}$$

2.2. Solution for the lower substrate

Similarly, the dynamic equation of SH-wave in Voigt-type viacoelastic orthotropic functionally graded half-space under the initial stress is

$$\frac{\partial\tau_{12}^2}{\partial x}+\frac{\partial\tau_{23}^2}{\partial x}-P_2\frac{\partial w_z}{\partial x}=\rho_2\frac{\partial^2 v_2}{\partial t^2} \tag{19}$$

By the means of Eqs. (1) and (6), the equation of motion given by Eq. (19) becomes

$$\frac{\partial}{\partial x}\left[\left\{\left(\mu_{66}^{12}+\eta_{66}^{12}\frac{\partial}{\partial t}\right)+\left(1+\frac{\partial}{\partial t}\right)\varepsilon(z-H)^2\right\}\frac{\partial v_2}{\partial x}\right]+\frac{\partial}{\partial z}\left[\left\{\left(\mu_{44}^{12}+\eta_{44}^{12}\frac{\partial}{\partial t}\right)+\left(1+\frac{\partial}{\partial t}\right)\varepsilon(z-H)^2\right\}\frac{\partial v_2}{\partial z}\right]$$
$$-\left(\frac{P_{12}+\varepsilon(z-H)^2}{2}\right)\frac{\partial^2 v_2}{\partial x^2}=\left(\rho_{12}+\varepsilon(z-H)^2\right)\frac{\partial^2 v_2}{\partial t^2} \tag{20}$$

Now again assuming $v_2=v_2(x,z)e^{i\omega t}$, we have

$$\left(\frac{\bar{\mu}_{62}}{\bar{\mu}_{42}}-\frac{P_{12}}{2\bar{\mu}_{42}}\right)\frac{\partial^2 v_2}{\partial x^2}+\frac{\partial^2 v_2}{\partial z^2}+\frac{\rho_{12}\omega^2}{\bar{\mu}_{42}}v_2=\frac{-\varepsilon}{\bar{\mu}_{42}}\left[(z-H)^2\left(\frac{1}{2}+i\omega\right)\frac{\partial^2 v_2}{\partial x^2}\right.$$
$$\left.+2(z-H)(1+i\omega)\frac{\partial v_2}{\partial z}+(z-H)^2(1+i\omega)\frac{\partial^2 v_2}{\partial z^2}+(z-H)^2\omega^2 v_2\right] \tag{21}$$

where

$$\bar{\mu}_{62}=\mu_{66}^{12}+i\omega\eta_{66}^{12}\quad\text{and}\quad\bar{\mu}_{42}=\mu_{44}^{12}+i\omega\eta_{44}^{12}$$

Now by using the Fourier transform in Eq. (21), we obtain

$$\frac{d^2\bar{V}_2}{dz^2}-\kappa_2^2\bar{V}_2=4\pi\sigma_2(z) \tag{22}$$

where

$$\kappa_2^2=\left(\frac{\bar{\mu}_{62}}{\bar{\mu}_{42}}-\frac{P_{12}}{2\bar{\mu}_{42}}\right)\xi^2-\lambda_2^2,\qquad \lambda_2^2=\frac{\rho_{12}\omega^2}{\bar{\mu}_{42}} \tag{23}$$

$$4\pi\sigma_2(z)=\frac{-\varepsilon}{\bar{\mu}_{42}}\left[(z-H)^2(1+i\omega)\frac{d^2\bar{V}_2}{dz^2}+2(z-H)(1+i\omega)\frac{d\bar{V}_2}{dz}-(z-H)^2\left\{\xi^2\left(\frac{1}{2}+i\omega\right)-\omega^2\right\}\bar{V}_2\right] \tag{24}$$

3. Boundary conditions and frequency equation

The stresses and displacements of the medium and substrate are continuous; and surface of the upper medium is traction free, then the boundary conditions for considered model are hold as follows:

$$\frac{d\bar{V}_1}{dz} = 0 \qquad \text{at} \qquad z = 0 \tag{25}$$

$$\bar{V}_1 = \bar{V}_2 \qquad \text{at} \qquad z = H \tag{26}$$

$$\bar{\mu}_{41}\cosh^2(\gamma z)\frac{d\bar{V}_1}{dz} = \bar{\mu}_{42}\frac{d\bar{V}_2}{dz} \qquad \text{at} \qquad z = H \tag{27}$$

With the aid of above boundary conditions (25)-(27), we solve Eqs. (16) and (22) by Green's function method. Let $G_1(z/z_0)$ be the Green's function for the viscoelastic orthotropic medium under the condition

$$\frac{dG_1}{dz} = 0 \quad at \quad z = 0, H$$

then the Eq. (16) must satisfy $G_1(z/z_0)$ as

$$\frac{d^2G_1(z/z_0)}{dz^2} - \kappa_1^2 G_1(z/z_0) = \delta(z - z_0) \tag{28}$$

here, z_0 is a point in the bounded layer.

Multiplying Eqs. (28) and (16) by $\bar{V}_1(z)$ and $G_1(z/z_0)$, respectively, then subtracting and further integrating with respect to z over $0 \le z \le H$, we get

$$G_1(H/z_0)\left[\frac{d\bar{V}_1}{dz}\right]_{z=H} = \frac{2}{\bar{\mu}_{41}\cosh(\gamma H)}G_1(H/z_0) - \bar{V}_1(z) \tag{29}$$

Replacing z_0 by z and applying the symmetry properties of Green's function, we get from equation (29) as

$$\bar{V}_1(z) = \frac{2}{\bar{\mu}_{41}\cosh(\gamma H)}G_1(z/H) - G_1(z/H)\left[\frac{d\bar{V}_1}{dz}\right]_{z=H} \tag{30}$$

Similarly, if $G_2(z/z_0)$ be Green's function associated with lower substrate, satisfying the equation

$$\frac{d^2G_2(z/z_0)}{dz^2} - \kappa_2^2 G_2(z/z_0) = \delta(z - z_0) \tag{31}$$

under the condition

$$\frac{dG_2}{dz} = 0 \quad \text{at} \quad z = H \;\&\; z \to \infty$$

In similar manner, we get

$$\bar{V}_2(z) = G_2(z/H)\left[\frac{d\bar{V}_2}{dz}\right]_{z=H} + \int_H^\infty 4\pi\sigma_2(z_0)G_2(z/z_0)dz_0 \tag{32}$$

By means of the condition $\bar{V}_1(H) = \bar{V}_2(H)$, we obtain from Eqs. (30) and (32)

$$\frac{2}{\bar{\mu}_{41}\cosh(\gamma H)}G_1(H/H) - G_1(H/H)\left[\frac{d\bar{V}_1}{dz}\right]_{z=H} = G_2(H/H)\left[\frac{d\bar{V}_2}{dz}\right]_{z=H} + \int_H^\infty 4\pi\sigma_2(z_0)G_2(H/z_0)dz_0 \tag{33}$$

Applying the boundary condition (27) in Eq. (33), we get

$$\left[\frac{d\bar{V}_1}{dz}\right]_{z=H} = \frac{\left(2/(\bar{\mu}_{41}\cosh(\gamma H))\right)G_1(H/H)}{G_1(H/H) + \frac{\bar{\mu}_{41}\cosh^2(\gamma H)}{\bar{\mu}_{42}}G_2(H/H)} - \frac{\int_H^\infty 4\pi\sigma_2(z_0)G_2(H/z_0)dz_0}{G_1(H/H) + \frac{\bar{\mu}_{41}\cosh^2(\gamma H)}{\bar{\mu}_{42}}G_2(H/H)} \tag{34}$$

Similarly, we have

$$\left[\frac{d\bar{V}_2}{dz}\right]_{z=H} = \frac{\left(2/(\bar{\mu}_{41}\cosh(\gamma H))\right)G_1(H/H)}{G_2(H/H) + \frac{\bar{\mu}_{42}}{\bar{\mu}_{41}\cosh^2(\gamma H)}G_1(H/H)} - \frac{\int_H^\infty 4\pi\sigma_2(z_0)G_2(H/z_0)dz_0}{G_2(H/H) + \frac{\bar{\mu}_{42}}{\bar{\mu}_{41}\cosh^2(\gamma H)}G_1(H/H)} \tag{35}$$

Putting the value of $\left[\frac{d\bar{V}_1}{dz}\right]_{z=H}$ and $4\pi\sigma_2(z_0)$ from Eqs. (34) and (24) into Eq. (30) respectively, we get

$$\begin{aligned}\bar{V}_1(z) = &\frac{2\cosh(\gamma H)G_1(z/H)G_2(H/H)}{\bar{\mu}_{42}G_1(H/H)+\bar{\mu}_{41}\cosh^2(\gamma H)G_2(H/H)} - \frac{\varepsilon G_1(z/H)}{\bar{\mu}_{42}G_1(H/H)+\bar{\mu}_{41}\cosh^2(\gamma H)G_2(H/H)}\\ &\times\int_H^\infty\left[(z_0-H)^2(1+i\omega)\frac{d^2\bar{V}_2}{dz_0^2}+2(z_0-H)(1+i\omega)\frac{d\bar{V}_2}{dz_0}-(z_0-H)^2\left\{\xi^2\left(\frac{1}{2}+i\omega\right)-\omega^2\right\}\bar{V}_2\right]G_2(H/z_0)dz_0\end{aligned} \tag{36}$$

Now, using Eqs. (35) and (24) in Eq. (32), we have

$$\begin{aligned}\bar{V}_2(z) = &\frac{2\cosh(\gamma H)G_1(H/H)G_2(z/H)}{\bar{\mu}_{42}G_1(H/H)+\bar{\mu}_{41}\cosh^2(\gamma H)G_2(H/H)} + \frac{\varepsilon\bar{\mu}_{41}\cosh^2(\gamma H)G_2(z/H)}{\bar{\mu}_{42}\left[\bar{\mu}_{42}G_1(H/H)+\bar{\mu}_{41}\cosh^2(\gamma H)G_2(H/H)\right]}\\ &\times\int_H^\infty\left[(z_0-H)^2(1+i\omega)\frac{d^2\bar{V}_2}{dz_0^2}+2(z_0-H)(1+i\omega)\frac{d\bar{V}_2}{dz_0}-(z_0-H)^2\left\{\xi^2\left(\frac{1}{2}+i\omega\right)-\omega^2\right\}\bar{V}_2\right]G_2(H/z_0)dz_0\\ &-\frac{\varepsilon}{\bar{\mu}_{42}}\int_H^\infty\left[(z_0-H)^2(1+i\omega)\frac{d^2\bar{V}_2}{dz_0^2}+2(z_0-H)(1+i\omega)\frac{d\bar{V}_2}{dz_0}-(z_0-H)^2\left\{\xi^2\left(\frac{1}{2}+i\omega\right)-\omega^2\right\}\bar{V}_2\right]G_2(z/z_0)dz_0\end{aligned} \tag{37}$$

Applying first-order approxmation in Eq. (37), we have

$$\bar{V}_2(z) = \frac{2\cosh(\gamma H)G_1(H/H)G_2(z/H)}{\bar{\mu}_{42}G_1(H/H)+\bar{\mu}_{41}\cosh^2(\gamma H)G_2(H/H)} \tag{38}$$

Eq. (38) gives the displacement for the orthotropic viscoelastic substrate, if it is considered as homogeneous.

Substituting the value of $\bar{V}_2(z)$ in Eq. (36), we obtained

$$\begin{aligned}\bar{V}_1(z) = &\frac{2\cosh(\gamma H)G_1(z/H)G_2(H/H)}{\bar{\mu}_{42}G_1(H/H)+\bar{\mu}_{41}\cosh^2(\gamma H)G_2(H/H)} - \frac{2\varepsilon\cosh(\gamma H)G_1(z/H)G_1(H/H)}{\left[\bar{\mu}_{42}G_1(H/H)+\bar{\mu}_{41}\cosh^2(\gamma H)G_2(H/H)\right]^2}\\ &\times\int_H^\infty\left[\begin{array}{l}(z_0-H)^2(1+i\omega)\dfrac{d^2G_2(z_0/H)}{dz_0^2}+2(z_0-H)(1+i\omega)\dfrac{dG_2(z_0/H)}{dz_0}\\ -(z_0-H)^2\left\{\xi^2\left(\dfrac{1}{2}+i\omega\right)-\omega^2\right\}G_2(z_0/H)\end{array}\right]G_2(H/z_0)dz_0\end{aligned} \tag{39}$$

In order to find the elastic displacement $\bar{V}_1(z)$ associated with the upper layer influenced by a unit impulsive force, we need to compute the value of $G_2(z/H)$ and $G_1(z/H)$.

Constructing $G_1(z/z_0)$ and $G_2(z/z_0)$ from equations (28) and (31), respectively, we have

$$G_1(z/z_0) = -\frac{1}{2\kappa_1}\left[e^{-\kappa_1|z-z_0|}+\frac{e^{\kappa_1 z}\left(e^{-\kappa_1(H+z_0)}+e^{-\kappa_1(H-z_0)}\right)}{e^{\kappa_1 H}-e^{-\kappa_1 H}}+\frac{e^{-\kappa_1 z}\left(e^{-\kappa_1(H-z_0)}+e^{-\kappa_1(H-z_0)}\right)}{e^{\kappa_1 H}-e^{-\kappa_1 H}}\right] \tag{40}$$

and

$$G_2(z/z_0) = -\frac{1}{2\kappa_2}\left[e^{-\kappa_2|z-z_0|}+e^{-\kappa_2(z+z_0-2H)}\right] \tag{41}$$

Substituting Eqs. (40) and (41) in Eq. (39), we have

$$\bar{V}_1(z) = \frac{-2\cosh(\gamma H)(e^{\kappa_1 z}+e^{-\kappa_1 z})}{E_1+F_1}\times\left[1+\frac{\varepsilon\left(e^{\kappa_1 H}+e^{-\kappa_1 H}\right)}{E_1+F_1}\left\{\left(\frac{2\bar{\mu}_{42}(1+i2\omega)}{2\bar{\mu}_{62}-P_{12}}-1\right)+\frac{1}{\kappa_2^2}\left(\frac{2\bar{\mu}_{42}(1+i2\omega)}{2\bar{\mu}_{62}-P_{12}}\lambda_2^2-2\omega^2\right)\right\}\right] \tag{42}$$

where

$$E_1 = \bar{\mu}_{41}\cosh^2(\gamma H)\kappa_1\left(e^{\kappa_1 H}-e^{-\kappa_1 H}\right) \quad \text{and} \quad F_1 = \bar{\mu}_{42}\kappa_2\left(e^{\kappa_1 H}+e^{-\kappa_1 H}\right)$$

Eq. (42) can be approximated if the higher powers of ε is neglected,

$$\bar{V}_1(z) = \frac{-2\cosh(\gamma H)(e^{\kappa_1 z}+e^{-\kappa_1 z})}{E_1+F_1-\varepsilon(e^{\kappa_1 H}+e^{-\kappa_1 H})\left\{\left(\frac{2\bar{\mu}_{42}(1+i2\omega)}{2\bar{\mu}_{62}-P_{12}}-1\right)+\frac{1}{\kappa_2^2}\left(\frac{2\bar{\mu}_{42}(1+i2\omega)}{2\bar{\mu}_{62}-P_{12}}\lambda_2^2-2\omega^2\right)\right\}} \tag{43}$$

Taking inverse Fourier transform in Eq. (43), we get

$$V_1(z) = -2\int_{-\infty}^{\infty}\frac{\cosh(\gamma H)(e^{\kappa_1 z}+e^{-\kappa_1 z})e^{-i\xi x}d\xi}{E_1+F_1-\varepsilon(e^{\kappa_1 H}+e^{-\kappa_1 H})\left\{\left(\frac{2\bar{\mu}_{42}(1+i2\omega)}{2\bar{\mu}_{62}-P_{12}}-1\right)+\frac{1}{\kappa_2^2}\left(\frac{2\bar{\mu}_{42}(1+i2\omega)}{2\bar{\mu}_{62}-P_{12}}\lambda_2^2-2\omega^2\right)\right\}} \tag{44}$$

Using Eq. (14) into Eq. (44), we have

$$v_1(z) = -2\int_{-\infty}^{\infty} \frac{(\cosh(\gamma H)/\cosh(\gamma z))(e^{\kappa_1 z}+e^{-\kappa_1 z})e^{-i\xi x}d\xi}{E_1+F_1-\varepsilon(e^{\kappa_1 H}+e^{-\kappa_1 H})\left\{\left(\frac{2\bar{\mu}_{42}(1+i2\omega)}{2\bar{\mu}_{62}-P_{12}}-1\right)+\frac{1}{\kappa_2^2}\left(\frac{2\bar{\mu}_{42}(1+i2\omega)}{2\bar{\mu}_{62}-P_{12}}\lambda_2^2-2\omega^2\right)\right\}} \tag{45}$$

To get the frequency equation of shear wave, we have to make the denominator of above equation (45) to be zero

$$E_1+F_1-\varepsilon(e^{\kappa_1 H}+e^{-\kappa_1 H})\left\{\left(\frac{2\bar{\mu}_{42}(1+i2\omega)}{2\bar{\mu}_{62}-P_{12}}-1\right)+\frac{1}{m_2^2}\left(\frac{2\bar{\mu}_{42}(1+i2\omega)}{2\bar{\mu}_{62}-P_{12}}\lambda_2^2-2\omega^2\right)\right\}=0 \tag{46}$$

After replacing ξ by k in Eq. (46), we have

$$\Gamma(k_1,c)=\tanh(H\kappa_1)+\frac{2\kappa_2\bar{\mu}_{42}+2\varepsilon\left(1+\frac{2\omega^2}{\kappa_2^2}+\frac{2\left(\kappa_2^2+\lambda_2^2\right)\bar{\mu}_{42}(1+2i\omega)}{\kappa_2^2(P_{12}-2\bar{\mu}_{62})}\right)}{2\kappa_1\bar{\mu}_{41}\cosh^2(\gamma H)}=0 \tag{47}$$

Eq. (47) represents the wave-velocity equation of SH-waves in pre-stressed orthotropic viscoelastic FGM layer overlying pre-stressed orthotropic viscoelastic FGM substrate under the influence of point source.

4. Particular cases and validation

Case 4.1: *Homogeneous orthotropic viscoelastic FGM medium over homogeneous orthotropic viscoelastic FGM half-space*

when in the assumed layered structure both medium and substrate is considered to be homogeneous with stress free i.e. $\gamma\to 0$, $\varepsilon\to 0$, $P_{11}\to 0$, $P_{12}\to 0$, then Eq. (47) reduces to

$$\tan\left(k_1H\sqrt{\frac{c^2\rho_{11}}{\mu_{44}^{11}+i\omega\eta_{44}^{11}}-\frac{\mu_{66}^{11}+i\omega\eta_{66}^{11}}{\mu_{44}^{11}+i\omega\eta_{44}^{11}}}\right)=\frac{(\mu_{44}^{12}+i\omega\eta_{44}^{12})\sqrt{\frac{\mu_{66}^{12}+i\omega\eta_{66}^{12}}{\mu_{44}^{12}+i\omega\eta_{44}^{12}}-\frac{c^2\rho_{11}}{\mu_{44}^{12}+i\omega\eta_{44}^{12}}}}{(\mu_{44}^{11}+i\omega\eta_{44}^{11})\sqrt{\frac{c^2\rho_{11}}{\mu_{44}^{11}+i\omega\eta_{44}^{11}}-\frac{\mu_{66}^{11}+i\omega\eta_{66}^{11}}{\mu_{44}^{11}+i\omega\eta_{44}^{11}}}}} \tag{48}$$

Eq. (48) is the dispersion equation for SH-waves propagation in homogeneous orthotropic viscoelastic medium lying over homogeneous orthotropic viscoelastic substrate.

Case 4.2: *Orthotropic medium over orthotropic substrate*

when in the assumed layered structure both medium and substrate is considered to be viscous free i.e $\eta_{ij}^{11}\to 0, \eta_{ij}^{12}\to 0$, then Eq. (48) transforms to

$$\tan\left(k_1H\sqrt{\frac{c^2\rho_{11}}{\mu_{44}^{11}}-\frac{\mu_{66}^{11}}{\mu_{44}^{11}}}\right)=\frac{\mu_{44}^{12}\sqrt{\frac{\mu_{66}^{12}}{\mu_{44}^{12}}-\frac{c^2\rho_{11}}{\mu_{44}^{12}}}}{\mu_{44}^{11}\sqrt{\frac{c^2\rho_{11}}{\mu_{44}^{11}}-\frac{\mu_{66}^{11}}{\mu_{44}^{11}}}} \tag{49}$$

Eq. (49) is the dispersion equation for SH-waves propagation in orthotropic medium lying over orthotropic half-space.

Case 4.3:*Isotropic medium over homogeneous half-space*

when in the assumed layered structure both medium and half-space is considered to be isotropic elastic medium with rigidity μ_1 (i.e.$\mu_{44}^{11}\to\mu_{66}^{11}\to\mu_1$) associated with the layer and μ_2 (i.e.$\mu_{44}^{12}\to\mu_{66}^{12}\to\mu_2$) associated with the half-space, then Eq. (49) converts to

$$\tan\left(k_1H\sqrt{\frac{c^2}{\beta_1^2}-1}\right)=\frac{\mu_2\sqrt{1-\frac{c^2}{\beta_2^2}}}{\mu_1\sqrt{\frac{c^2}{\beta_1^2}-1}} \tag{50}$$

where

$$\beta_1=\sqrt{\frac{\mu_1}{\rho_1}}\quad\text{and}\quad\beta_2=\sqrt{\frac{\mu_2}{\rho_2}}$$

Eq. (50) represents the well-known pre-established classical relation of Love wave in an isotropic layer lying over homogeneous half-space, which coincides the results obtained by Ewing[1] and Love[2].

5. Graphical observation and discussions

Graphical observation based on the obtained results in the form of wave-velocity Eq. (47) are provided to demonstrate the influence of heterogeneity and viscoelasticity associated with the medium and substrate in the both presence and absence of initial stress on phase velocity (c/β_1) and attenuation coefficient ($Log(\delta)$) by taking into account the Re $[\Gamma(k_1, c)]$

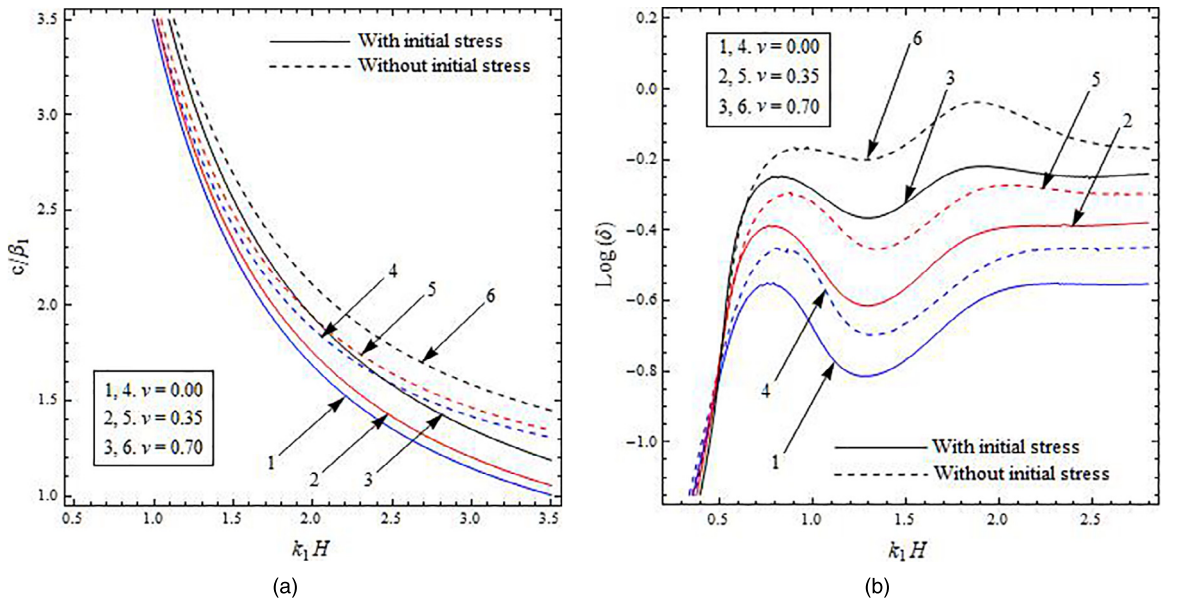

Fig. 2. Variations of (a) phase velocity c/β_1 and (b) attenuation coefficient $Log(\delta)$ against wave number k_1H for different values of viscoelasticity $\nu = \omega\,\eta_{44}^{11}/\mu_{44}^{11}$ of the layer.

and Im $[\Gamma(k_1, c)]$ respectively. The parameters $\nu = \omega\eta_{44}^{11}/\mu_{44}^{11}$ and $\tilde{\nu} = \omega\eta_{44}^{12}/\mu_{44}^{12}$ are denoting the non-dimensional viscoelasticity of the upper layer and half-space respectively. Likewise, the parameters γ/k_1 and $\varepsilon/(k_1\mu_{44}^{12})$ are denoting the non-dimensional heterogeneity of the upper layer and half-space, respectively. We have taken the following data for numerical work from Yu et al.[30]:

For viscoelastic functionally graded (FGM) bounded layer:

$$\mu_{44}^{11} = 7.8 \text{ GPa}, \quad \mu_{66}^{11} = 3.9 \text{ GPa}, \quad \eta_{44}^{11} = 0.0042 \text{ GPa ms}, \quad \eta_{66}^{11} = 0.0034 \text{ GPa ms}, \quad \rho_1 = 1.595 \text{ g/cm}^3$$

For viscoelastic functionally graded (FGM) lower half-space:

$$\mu_{44}^{12} = 6.15 \text{ GPa}, \quad \mu_{66}^{12} = 3.32 \text{ GPa}, \quad \eta_{44}^{12} = 0.02 \text{ GPa ms}, \quad \eta_{66}^{12} = 0.009 \text{ GPa ms}, \quad \rho_2 = 1.5 \text{ g/cm}^3$$

The Wolfram Mathematica 9.0 software has been used for computational work and acquired results are depicted graphically. In the under mentioned figures, non-dimensional wave number k_1H represents the horizontal axis, whereas a non-dimensional attenuation coefficient $Log(\delta)$ and phase velocity c/β_1 represent the vertical axis. In each of the figure, first subfigure (a) delineates the impact of influencing parameters on the phase velocity of SH-wave while the second subfigure (b) stand for the influence of same on the attenuation coefficient. The solid line curves (Curves 1, 2, and 3) in each of the subfigures illustrate the case when medium is under the influence of initial stress, while the dashed line curves (Curves 4, 5, 6) in the subfigures represent the case of absence of initial stress. The detailed discussions on figures are as follows:

5.1. Effect of viscoelasticity on phase velocity and attenuation coefficient

Fig. 2 (a) and (b) exhibit the influence of viscoelasticity (ν) associated with the upper medium on the phase velocity and attenuation coefficient against dimensionless wave number respectively. Different values of viscoelastic parameter (ν) are taken into consideration to study its influence on attenuation as well as phase velocity are as 0.00, 0.35, 0.70. Curves 1 and 4 of these figures represent that the bounded medium is viscous free (i.e., $\nu = 0$). Following observations and effects are marked as:

- The phase velocity of SH-wave gets discouraged with the rising value of wave number. However, the attenuation coefficient gets encouraged dramatically $k_1H \leq 0.7$, decreases monotonically for the wave number $k_1H \leq 1.2$, again increases and at last follow a constant trend for the higher values of wave number. The same influence of wave number on attenuation coefficient as well as phase velocity are reported for the case of both the presence and absence of initial stresses.
- Both attenuation coefficient and phase velocity of SH-wave get encouraged due to each rise in the mentioned value of viscoelastic parameter (ν). In addition to that, the attenuation as well as phase velocity of SH-wave are minimum when the viscoelasticity is absent with initial stress in upper medium and are maximum when the viscoelasticity is present without initial stress.
- Both phase velocity and attenuation curves are much closer in the lower region of wave number as compared to the higher region of wave number for various values of viscoelasticity which suggests that the presence of viscoelasticity in

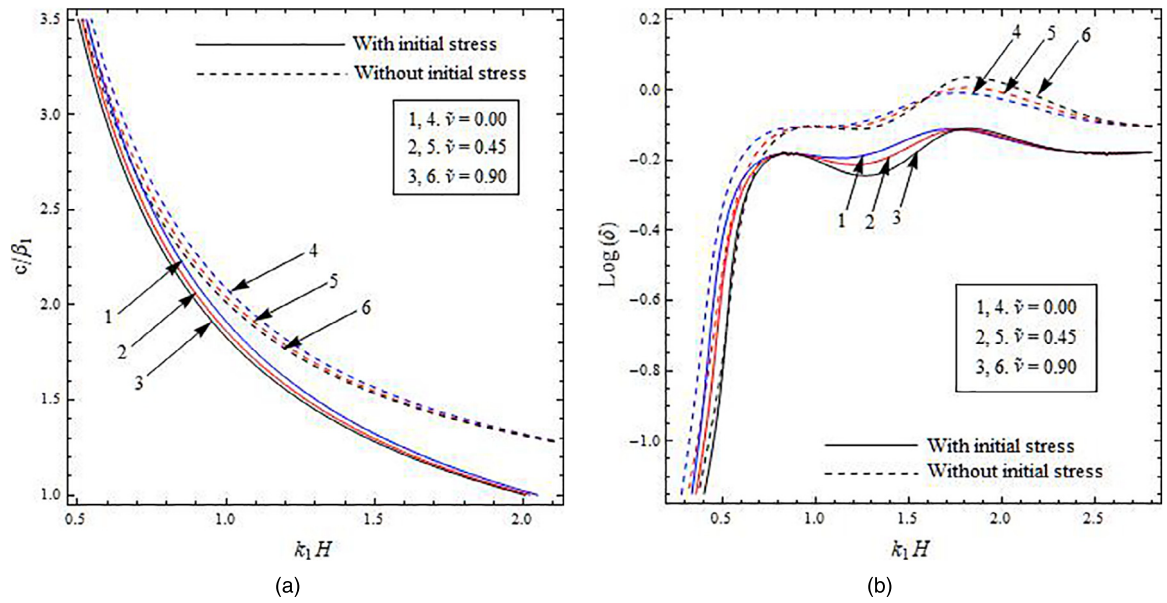

Fig. 3. Variations of (a) phase velocity c/β_1 and (b) attenuation coefficient $Log(\delta)$ against wave number $k_1 H$ for different values of viscoelasticity $\tilde{v} = \omega\ \eta_{44}^{12}/\mu_{44}^{12}$ of the half-space.

the upper layer has most prominent influence in the higher range of wave number and a little influence in lower range of wave number for the case of presence and absence of initial stress.

The phase velocity and attenuation coefficient are plotted against dimensionless wave number for various values of viscoelasticity ($\tilde{v}$) associated with substrate in Fig. 3(a) and (b) respectively. To serve the purpose, values of viscoelastic parameter $\tilde{v}$ are taken as 0.00, 0.45, 0.90. Curves 1 and 4 explain the lower half-space is viscous free (i.e., $\tilde{v} = 0$). Following observations can be noted from these figures:

- The phase velocity curves follow a same trend with respect to increasing value of wave number for the mentioned values of $\tilde{v}$ as it is observed for different prescribed values of v. However, it also can be noted that attenuation coefficient for the rising wave number also follow the same trend as for the v. More accurately, the attenuation coefficient increases for the wave number $k_1 H \leq 0.9$, thereafter it decreases monotonically for a while $k_1 H \leq 1.5$, again increases slightly for the wave number $k_1 H \leq 2$ and become constant after a small decrement. These trends are observed for the presence and absence of initial stress in the considered medium.
- A disfavouring behaviour on the phase velocity is marked for the mounting value of viscoelastic parameter ($\tilde{v}$). On the contrary to this, the increase in viscoelastic parameter $\tilde{v}$ discourages the attenuation coefficient of SH-wave for the wave number $k_1 H \leq 1.8$ (in the presence of initial stress) and wave number $k_1 H \leq 1.6$ (in the absence of initial stress). However, the nature of the curves get reversed for wave number $k_1 H \geq 1.8$ and $k_1 H \geq 1.6$ in the presence and absence of initial stress, respectively.
- Apart from that, the influence of the viscoelastic parameter on the attenuation as well as phase velocity are more in the absence of initial stress than in the presence of initial stress.

Surface plots in Fig. 4(a) and (b) elucidate on the combined variation of phase velocity and attenuation coefficient respectively, with respect to wave number; and viscoelasticity of bounded medium for the traversal of seismic shear waves in viscoelastic orthotropic FGM composite layered structure with initial stress. When the fixed values of $\tilde{v}$, γ/k_1 and $\varepsilon/(k_1 \mu_{44}^{12})$ are contracted as 0.4, 0.3 and 0.6. Similarly Fig. 5(a) and (b) show the joint variation of phase velocity and attenuation coefficient respectively, with respect to wave number; and viscoelasticity of lower substrate.

5.2. Effect of heterogeneities on phase velocity and attenuation coefficient

Fig. 6 (a) and (b) elucidate the variation of phase velocity profile and attenuation with respect to wave number for various distinct values of heterogeneity parameter γ/k_1 associated with the layer as 0, 0.3 and 0.6. In both figures, curves 1 and 4 represent the case when there is no heterogeneity present in the layer (i.e., $\gamma/k_1 = 0$). The remarks drawn from the two figures are as follows:

- A monotonic decrease in the phase velocity with respect to increase in wave number is observed while a sharp increase in the attenuation coefficient for the wave number $k_1 H \leq 0.7$ is manifested, then a decreasing behaviour of attenua-

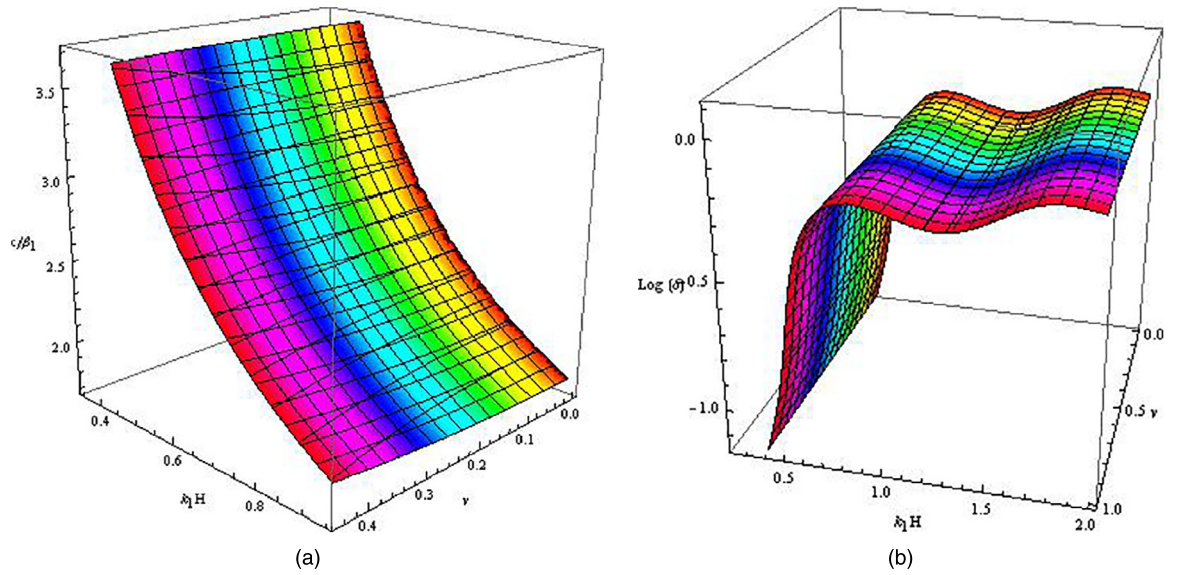

Fig. 4. Surface plots showing combined variation of (a) phase velocity c/β_1 and (b) attenuation coefficient $Log(\delta)$ against wave number k_1H and viscoelasticity $v = \omega\ \eta_{44}^{11}/\mu_{44}^{11}$ of the layer.

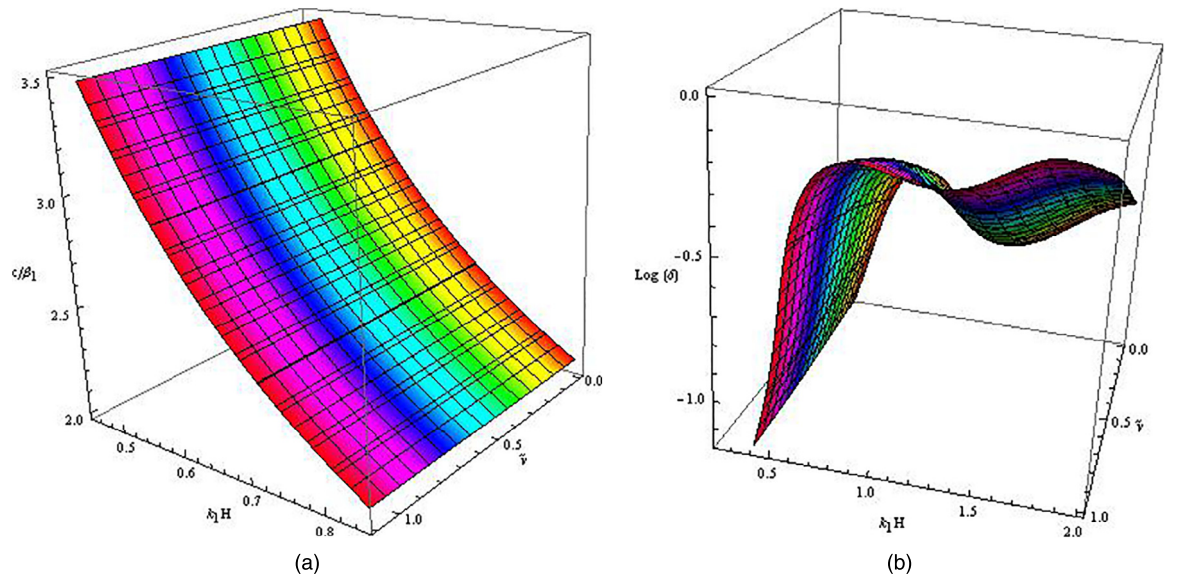

Fig. 5. Surface plots showing combined variation of (a) phase velocity c/β_1 and (b) attenuation coefficient $Log(\delta)$ against wave number k_1H and viscoelasticity $\tilde{v} = \omega\ \eta_{44}^{12}/\mu_{44}^{12}$ of the half-space.

tion coefficient is noticed for the higher range of wave number which is followed by a slight decrease due to further increment in the wave number. The trend is same for the case of both the presence and absence of initial stress.

- The heterogeneity associated with the upper medium favours both attenuation coefficient and phase velocity. However, more significant effect of heterogeneity parameter on attenuation coefficient is observed to be in the higher values of wave number as compared to that of the lower values of wave number. But, the influence of heterogeneity parameter is found to be uniform for the complete range of wave number.
- The curves in both the figures recommend that both the attenuation coefficient and phase velocity are minimum when there is no heterogeneity associated with upper layer in the presence of initial stress and are maximum when there is heterogeneity associated with upper layer in the absence of initial stress.

In order to show the influence of heterogeneity parameter $\varepsilon/(k_1\mu_{44}^{12})$ associated with the lower half-space, Fig. 7(a) and (b) is portrayed. The values of $\varepsilon/(k_1\mu_{44}^{12})$ have been considered as 0, 0.3 and 0.6. Curves 1 and 4 of both the figures

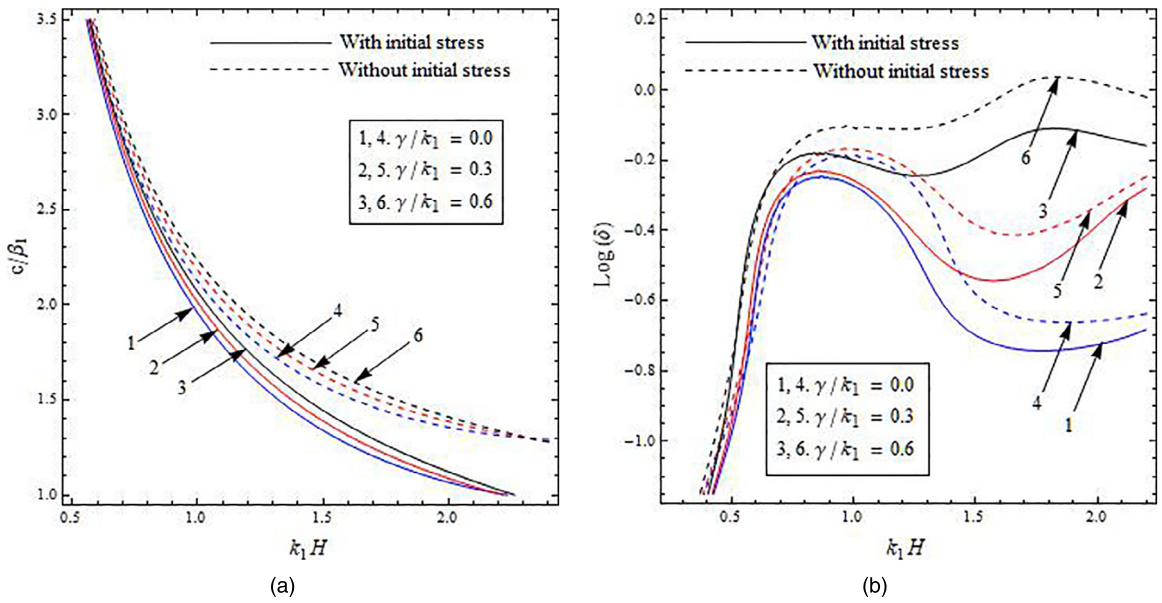

Fig. 6. Variations of (a) phase velocity c/β_1 and (b) attenuation coefficient $Log(\delta)$ against wave number k_1H for different values of heterogeneity parameter γ/k_1 of the layer.

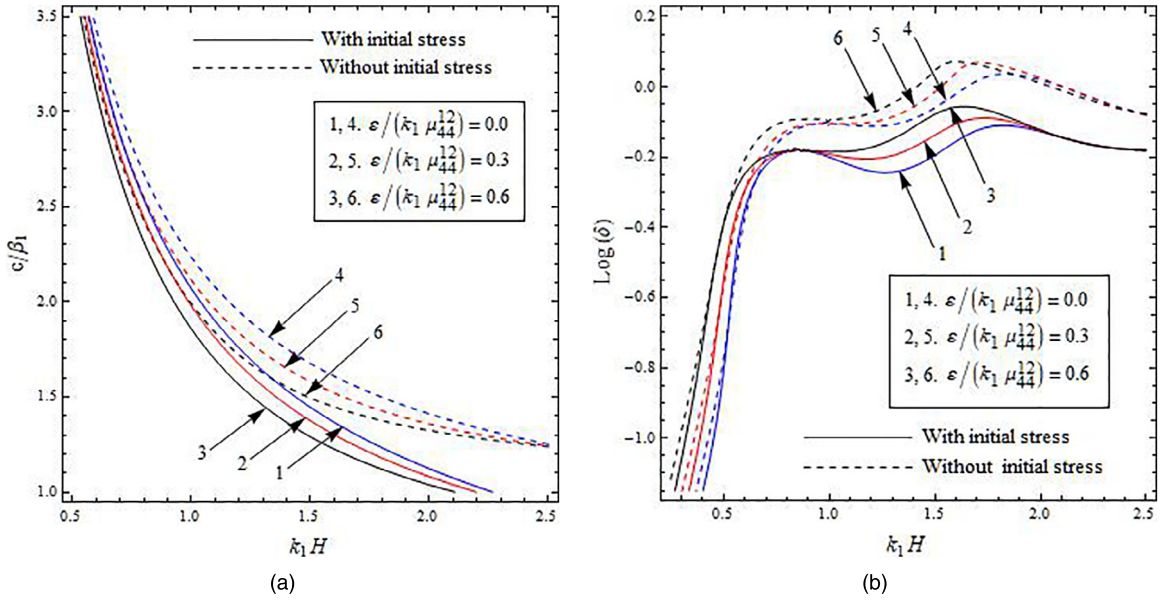

Fig. 7. Variations of (a) phase velocity c/β_1 and (b) attenuation coefficient $Log(\delta)$ against wave number k_1H for different values of heterogeneity parameter $\varepsilon/(k_1\mu_{44}^{12})$ of the half-space.

represent the case when there is no heterogeneity present in the lower half-space (i.e., $\varepsilon/(k_1\mu_{44}^{12}) = 0$). The noticeable observations of these figures are as follows:

- A similar nature of the phase velocity and attenuation coefficient with respect to wave number for distinct values of heterogeneity parameter $\varepsilon/(k_1\mu_{44}^{12})$ associated with the lower half-space is found as it is marked for the mentioned values γ/k_1.
- The heterogeneity present in the lower half-space diminishes the phase velocity for the entire range of wave number. A sharp increment in the attenuation coefficient is observed as we gradually increase the value of wave number and after that a slight downfall is perceived in the attenuation due to further increment in the values of wave number. Finally a slight enhancement and thereafter a steady nature in the pattern of attenuation coefficient is noticed with the increment of the higher range of wave number.

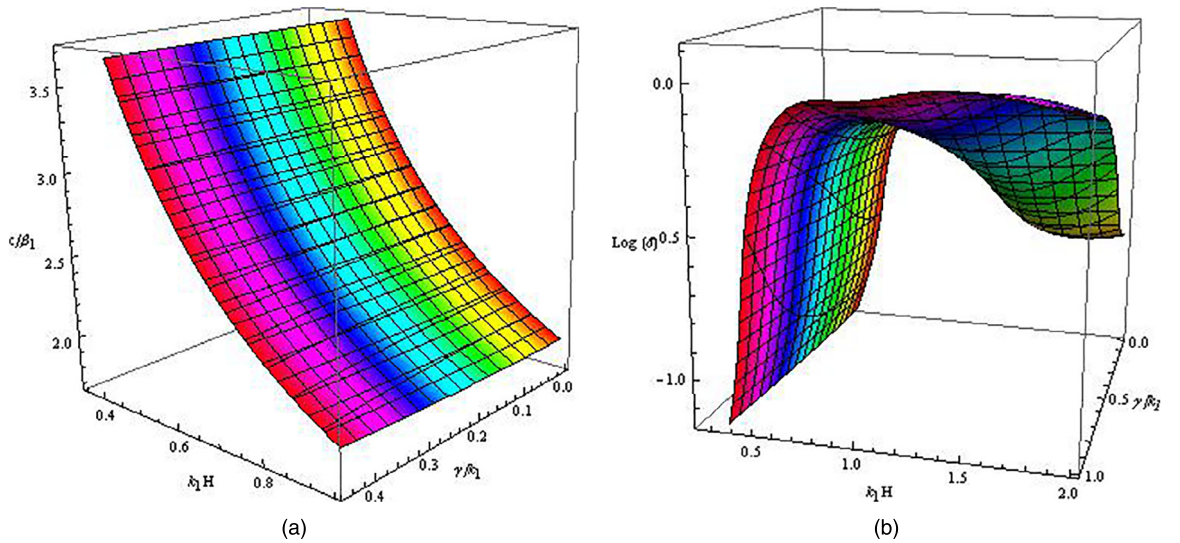

Fig. 8. Surface plots showing combined variation of (a) phase velocity c/β_1 and (b) attenuation coefficient $Log(\delta)$ against wave number k_1H and heterogeneity γ/k_1 of the layer.

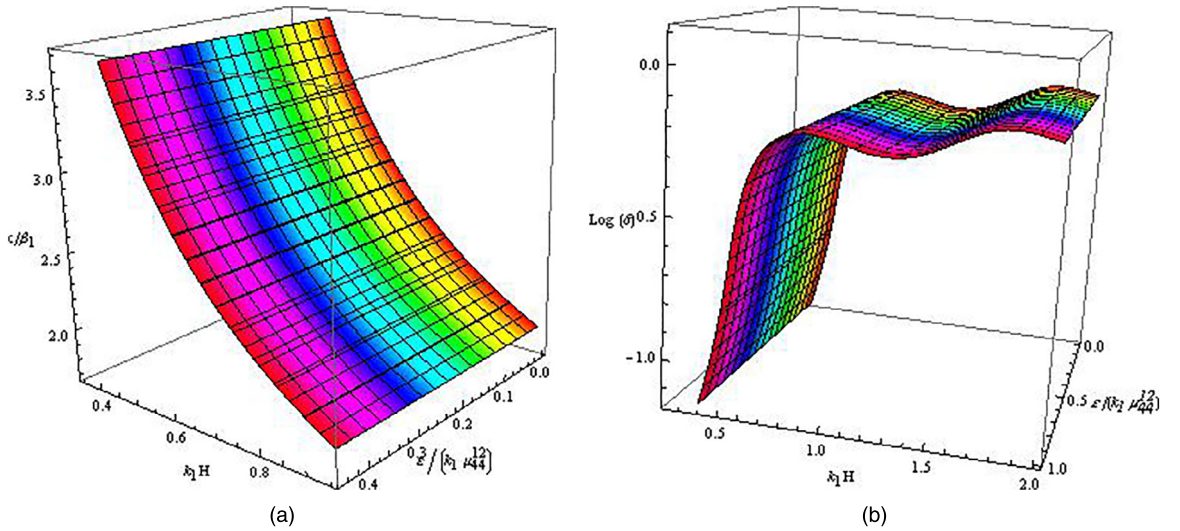

Fig. 9. Surface plots showing combined variation of (a) phase velocity c/β_1 and (b) attenuation coefficient $Log(\delta)$ against wave number k_1H and heterogeneity $\varepsilon/(k_1\mu_{44}^{12})$ of the half-space.

- From both the figures, we perceive that the attenuation of shear wave is minimum for that case when the lower half-space is homogeneous with initial stress while the phase velocity is same when the lower half-space is heterogeneity with initial stress.

The combined variation of phase velocity; and wave number against heterogeneity of the bounded medium and lower substrate are focused by means of surface plots in Figs. 8(a) and 9(a), when the seismic shear wave passes through viscoelastic orthotropic FGM composite layered structure with initial stress. However, Figs. 8(b) and 9(b) trace out the joint effect of attenuation coefficient; and wave number with respect to heterogeneity of the medium and substrate.

6. Conclusions

In this study, the traversal behaviour of SH-wave influenced by an impulsive point source in an orthotropic viscoelastic FGM medium lying over an orthotropic viscoelastic FGM substrate has been examined. With the aid of mathematical tools viz. Green's function and Fourier transform, complex form of velocity equation has been achieved in compact form. The obtained results are numerically computed using numerical data and are illustrated graphically. A prominent effect of the affecting parameters on the traversal behaviour of SH-wave has been reported. Moreover, the comparative study has been

accomplished in order to examine the influence of affecting parameters on the traversal behaviour of SH-wave for the presence and absence of initial stress in the considered media. Following are the major outcomes of the present study under assumed conditions:

- It is established that the phase velocity of SH-wave gets disfavoured with the growing wave number while the attenuation coefficient gets favoured initially with the increase in wave number followed by a disfavouring behaviour (for a small range of wave number) and become constant thereafter throughout the entire range of wave number.
- The viscoelasticity associated with the upper medium favours attenuation coefficient as well as phase velocity of seismic shear wave in a significant manner for the both the cases of presence and absence of initial stresses in the media. More accurately, the attenuation coefficient gets much substantially influenced due to viscoelasticity acting in the upper medium for the wave number ($k_1H_1 \geq 0.5$).
- The viscoelasticity associated with substrate favours phase velocity of seismic shear wave in the entire region of wave number. However, the presence of viscoelasticity in the lower substrate encourages the attenuation coefficient in the lower range of wave number, thereafter its effect become negligible on the attenuation coefficient for the higher wave number ($k_1H_1 \geq 2$). The influence of viscoelasticity on attenuation coefficient as well as phase velocity are same for the presence and absence of initial stress.
- The heterogeneity parameter associated with the upper medium has significant encouraging influence on the phase velocity of SH-wave in complete range of wave number. On contrary, attenuation coefficient of SH wave gets significantly favoured due to viscoelasticity associated with the upper medium in the higher region of wave number as compared to that of lower region of wave number.
- Phase velocity of SH-wave diminishes with rising value of heterogeneity parameter contained in the half-space while the attenuation coefficient increases. The minute study of the figures reveal that the phase velocity is discouraged considerably in the complete range of wave number, while the attenuation coefficient gets significantly disfavoured for the wave number ($k_1H_1 \leq 2$). The attenuation curves for different values of $\varepsilon/(k_1\mu_{44}^{12})$ is coincident for the higher values of wave number.
- It is worth mentioning that phase velocity as well as attenuation coefficient of SH-wave are comparatively more for the case when there is no initial stress acting in the upper and lower media than that for the case when initial stress is acting in both the media.

Observations made in the present theoretical framework may suggest a significant contribution to the problems of wave propagation, vibration and geophysical surveys through the Earth layered model with different material properties. Moreover, this result can be used as the first initial information for exploring the underground formations.

Funding source

This research did not receive any specific grant from funding agencies in the public, commercial, or not-for-profit sectors.

Acknowledgement

The authors would like to convey their heartfelt gratitude to Indian Institute of Technology (ISM), Dhanbad, Jharkhand-826004, India, for providing all necessary facilities to Mr. Raju Kumhar for this research work.

References

[1] W.M. Ewing, W.S. Jardetzky, F. Press, Elastic Waves in Layered Media, McGraw-Hill, New York, 1957.
[2] A.E.H. Love, Mathematical Theory of Elasticity, Cambridge University Press, Cambridge, 1920.
[3] D. Gubbins, Seismology and Plate Tectonics, Cambridge University Press, Cambridge, 1990.
[4] J. Pujol, Elastic Wave Propagation and Generation in Seismology, Cambridge University Press, Cambridge, 2003.
[5] P.C. Vinh, V.T.N. Anh, V.P. Thanh, Rayleigh waves in an isotropic elastic half-space coated by a thin isotropic elastic layer with smooth contact, Wave Motion 51 (3) (2014) 496–504.
[6] P.A. Gourgiotis, H.G. Georgiadis, Torsional and SH surface waves in an isotropic and homogenous elastic half-space characterized by the toupin mindlin gradient theory, Int. J. Solids Struct. 62 (2015) 217–228.
[7] S. Dutta, Love waves in a non-homogeneous internal stratum lying between two isotropic media, Geophysics 28 (1963) 156–160.
[8] B. Singh, Wave propagation in an initially stressed transversely isotropic thermoelastic solid half-space, Appl. Math. Comput. 217 (2) (2010) 705–715.
[9] H. Zhu, L. Zhang, J. Han, Y. Zhang, Love wave in an isotropic homogeneous elastic half-space with a functionally graded cap layer, Appl. Math. Comput. 231 (2014) 93–99.
[10] Y. Pang, J.X. Liu, Y.S. Wang, X.F. Zhao, Propagation of rayleigh-type surface waves in a transversely isotropic piezoelectric layer over a piezomagnetic half-space, J. Appl. Phys. 103 (2008) 074901.
[11] M. Destrade, Surface waves in orthotropic incompressible materials, J. Acoust. Soc. Am. 110 (2) (2001) 837–840.
[12] A.M. Abd-Alla, S.M. Ahmed, Propagation of love waves in a non-homogeneous orthotropic elastic layer under initial stress overlying semi-infinite medium, Appl. Math. Comput. 106 (2–3) (1999) 265–275.
[13] J.T. Wilson, Surface waves in a heterogeneous medium, Bull. Seismol. Soc. Am. 32 (4) (1942) 297–304.
[14] S. Dey, A.K. Gupta, S. Gupta, Torsional surface waves in non-homogeneous and anisotropic medium., J. Acoust. Soc. Am. 99 (5) (1996) 2737–2741.
[15] M.A. Biot, The influence of initial stress on elastic waves, J. Appl. Phys. 11 (8) (1940) 522–530.
[16] A. Saha, S. Kundu, S. Gupta, P.K. Vaishnav, Effect of irregularity on torsional surface waves in an initially stressed anisotropic porous layer sandwiched between homogeneous and non-homogeneous half-space, J. Earth Syst. Sci. 125 (4) (2016) 885–895.
[17] S. Kundu, S. Gupta, S. Manna, Propagation of g-type seismic waves in heterogeneous layer lying over an initially stressed heterogeneous half-space, Appl. Math. Comput. 234 (2014) 1–12.

[18] L.L. Ke, Y.S. Wang, Z.M. Zhang, Love waves in an inhomogeneous fluid saturated porous layered half-space with linearly varying properties, Soil Dyn. Earthq. Eng. 26 (6–7) (2006) 574–581.
[19] L.L. Ke, Y.S. Wang, Z.M. Zhang, Propagation of love waves in an inhomogeneous fluid saturated porous layered half-space with properties varying exponentially, J. Eng. Mech. 131 (12) (2005) 1322–1328.
[20] C.D. Wang, H.T. Chou, D.H. Peng, Love-wave propagation in an inhomogeneous orthotropic medium obeying the exponential and generalized power law models, Int. J. Geomech. 17 (7) (2017) 4017003.
[21] A.M. Abd-Alla, H.A.H. Hammad, S.M. Abo-Dahab, Rayleigh waves in a magnetoelastic half-space of orthotropic material under influence of initial stress and gravity field, Appl. Math. Comput. 154 (2) (2004) 583–597.
[22] J.M. Carcione, Wave propagation in anisotropic linear viscoelastic media: theory and simulated wavefields, Geophys. J. Int. 101 (1990) 739–750.
[23] R. Borcherdt, Rayleigh-type surface wave on a linear viscoelastic half-space., J. Acoust. Soc. Am. 54 (6) (1973) 1651–1653.
[24] J.M. Carcione, Rayleigh waves in isotropic viscoelastic media, Geophys. J. Int. 108 (2) (1992) 453–464.
[25] M. Maity, S. Kundu, D.K. Pandit, S. Gupta, Characteristics of torsional wave profiles in a viscous fiber-reinforced layer resting over a sandy half-space under gravity, Int. J. Geomech. 18 (7) (2018) 6018015.
[26] Y. Kong, J. Liu, G. Nie, Propagation characteristics of SH waves in a functionally graded piezomagnetic layer on PMN-0.29 PT single crystal substrate, Mech. Res. Commun. 73 (2016) 107–112.
[27] G.H. Paulino, Z.H. Jin, Correspondence principle in viscoelastic functionally graded materials, J. Appl. Mech. 68 (1) (2001) 129–132.
[28] J. Yu, C. Zhang, Effects of initial stress on guided waves in orthotropic functionally graded plates, Appl. Math. Model. 38 (2) (2014) 464–478.
[29] Z.H. Qian, F. Jin, K. Kishimoto, T. Lu, Propagation behavior of love waves in a functionally graded half-space with initial stress, Int. J. Solids Struct. 46 (6) (2009) 1354–1361.
[30] J.G. Yu, F.E. Ratolojanahary, J.E. Lefebvre, Guided waves in functionally graded viscoelastic plates, Compos. Struct. 93 (11) (2011) 2671–2677.
[31] D. Ren, X. Shen, C. Li, X. Cao, The fractional kelvin-voigt model for rayleigh surface waves in viscoelastic FGM infinite half space, Mech. Res. Commun. 87 (2018) 53–58.
[32] X.Y. Li, Z.K. Wang, S.H. Huang, Love waves in functionally graded piezoelectric materials, Int. J. Solids Struct. 41 (26) (2004) 7309–7328.
[33] Z.H. Qian, F. Jin, S. Hirose, Piezoelectric love waves in an FGPM layered structure, Mech. Adv. Mater. Struct. 18 (1) (2011) 77–84.
[34] J. Liu, Z.K. Wang, The propagation behavior of love waves in a functionally graded layered piezoelectric structure, Smart Mater. Struct. 14 (1) (2004) 137.
[35] P. Assari, M. Dehghan, A meshless discrete collocation method for the numerical solution of singular-logarithmic boundary integral equations utilizing radial basis functions, Appl. Math. Comput. 315 (2017) 424–444.
[36] P. Assari, M. Dehghan, A meshless galerkin scheme for the approximate solution of nonlinear logarithmic boundary integral equations utilizing radial basis functions, J. Comput. Appl. Math. 333 (2018) 362–381.
[37] P. Assari, M. Dehghan, Application of thin plate splines for solving a class of boundary integral equations arisen from Laplace's equations with nonlinear boundary conditions, Int. J. Comput. Math. 96 (1) (2019) 170–198.